Dynamically Orthogonal Differential Equations for Stochastic and Deterministic Reduced-Order Modeling of Ocean Acoustic Wave Propagation

Aaron Charous
Department of Mechanical Engineering
Massachusetts Institute of Technology
Cambridge, Massachusetts 02139
acharous@mit.edu

Pierre F.J. Lermusiaux
Department of Mechanical Engineering
Massachusetts Institute of Technology
Cambridge, Massachusetts 02139
pierrel@mit.edu

***Abstract*—Accurate and computationally efficient acoustic models are needed for varied marine applications. In this paper, we focus our attention on forward models, which are essential to inverse problems such as imaging and mapping. First, we introduce new dynamically orthogonal (DO) equations for the acoustic wave equation in full generality, allowing for stochastic and spatially heterogeneous parameters. These equations may be spatially discretized and integrated in time numerically. Alternatively, the DO equations may be discretized themselves, admitting a non-intrusive reduced-order approach to solve the stochastic wave equation. We demonstrate the latter with a test case of an acoustic pulse traveling through the ocean with an uncertain sound speed. Second, we adapt the spatially discrete DO approach, typically used to reduce the stochastic dimension, to efficient reduced-order modeling of deterministic 3D acoustic propagation. We solve the 3D parabolic wave equation and show that low-rank solutions rapidly converge to the full-rank solution. Together, these approaches offer novel ways to solve stochastic and deterministic problems with strong or weak scattering at a reduced computational cost.**

I. Introduction

Despite considerable efforts, the ocean remains largely unmapped; not only are there challenges due to the ocean's sheer size, but electromagnetic radiation is attenuated significantly in the water [1]. Hence, acoustic waves are used to collect data in the ocean, but this comes with its own set of challenges. First and foremost, the geoacoustic parameters of the ocean are spatially heterogeneous and often uncertain, making acoustic prediction and inversion quite challenging [2]–[11]. In this work, we take a first step in deriving and applying efficient reduced-order forward models for three-dimensional high-resolution ocean acoustic propagation [12], a key ingredient in the process of imaging [13], [14].

The dynamically orthogonal (DO) equations offer an instantaneously optimal set of equations to evolve a reduced-order model [15]. Given a time-varying stochastic field, we decompose the solution into time-varying, deterministic, spatially-varying modes and time-varying, stochastic coefficients. The DO equations were first developed for stochastic parabolic differential equations [16], and they have been applied to stochastic advection [17], stochastic fluid and ocean flows [18]–[21], and stochastic optimal path planning [22]–[25]. Most recently, DO equations were derived and employed using the stochastic parabolic (or paraxial) wave equation for stochastic ocean acoustics estimation and Bayesian inversion [26]–[28]. This works well for forward acoustic propagation at medium to low frequency, and, due to its parabolic nature, the PDE is computationally efficient to solve. However, for complex (and higher-frequency) propagation in range-dependent media that are especially important in scattering phenomena, we may need a more accurate forward model.

We introduce two novel ideas in this paper. In section II, we introduce new DO equations for the acoustic wave equation in full generality. These equations may be used to numerically solve a wave equation in $\mathbb{R}^d$ with stochastic and spatially heterogeneous coefficients. In section III, we also show how the dynamical low-rank approximation [29]–[31] may be applied to the stochastic acoustic wave equation, which is much less intrusive and abstracts away the need for explicitly computing new DO equations for each new PDE. In section IV, we show how the dynamical low-rank approximation may be applied to the deterministic 3D parabolic wave equation, yielding approximate reduced-order solutions of 3D waves very efficiently. We conclude in section V with some remarks on the aforementioned methods' efficacy as well as future research directions.

II. Spatially continuous and discrete DO equations for stochastic acoustic wave propagation

In this section, we derive DO equations for the stochastic acoustic wave equation with spatially heterogenous and stochastic attenuation, sound speed, and density. Consider the time-space wave equation in the form below.

$$c^2\rho\nabla\cdot\left(\frac{1}{\rho}\nabla p\right)-\alpha\frac{\partial p}{\partial t}+f=\frac{\partial^2 p}{\partial t^2} \tag{1}$$

where p denotes pressure, c sound speed, ρ density, and α attenuation, and f is a forcing function; these may all be

978-0-692-93559-0 ©2021 MTS

stochastic and spatially varying. To simplify the algebra, we make a variable transform. Letting $\phi \equiv \log \rho$, eq. (1) becomes,

$$c^2 \left(\nabla^2 p - \nabla\phi \cdot \nabla p\right) - \alpha \frac{\partial p}{\partial t} + f = \frac{\partial^2 p}{\partial t^2} \tag{2}$$

As is done in the symplectic case with a simpler wave equation [32], [33], we convert the hyperbolic PDE into a parabolic one by writing down the PDE in its phase space representation. Let $\Psi = (p, \frac{\partial p}{\partial t})^T$. The second-order PDE (2) may now be written as a system of first-order PDEs.

$$\frac{\partial \Psi}{\partial t} = \begin{pmatrix} 0 & 1 \\ c^2\left[\nabla^2 - \nabla\phi^T\nabla\right] & -\alpha \end{pmatrix} \Psi + \begin{pmatrix} 0 \\ f \end{pmatrix} \tag{3}$$

Now that the PDE is in parabolic form, we develop the corresponding DO equations. We assume Ψ, a stochastic field, may be decomposed into the mean of the field, $\overline{\Psi}$, as well as the superposition of the product of stochastic coefficients, ζ, and spatially-varying, deterministic modes, ψ [16]. This is a dynamic extension of the Karhunen-Loève expansion [34], [35].

$$\Psi(x,t;\eta) = \overline{\Psi}(x,t) + \sum_{i=1}^{\infty} \psi_i(x,t)\zeta_i(t;\eta) \tag{4}$$

Here, x and t are space and time, as usual, and η represents a simple event in the stochastic event space Ω. In a typical Galerkin sense, we substitute (4) into (12) and, following the procedure in [16] using the DO condition that $\langle \frac{\partial \psi_i}{\partial t}, \psi_j \rangle \quad \forall i,j$, we obtain differential equations for the mean, mode, and coefficients,

$$\begin{aligned} \frac{\partial \overline{\Psi}}{\partial t} &= \begin{pmatrix} 0 & 1 \\ \mathbb{E}[c^2]\nabla^2 - \mathbb{E}[c^2\nabla\phi]\cdot & -\mathbb{E}[\alpha] \end{pmatrix} \overline{\Psi} \\ &+ \sum_i \left[\begin{pmatrix} 0 & 0 \\ \mathbb{E}[c^2\zeta_i]\nabla^2 - \mathbb{E}[c^2\zeta_i\nabla\phi]\cdot\nabla & -\mathbb{E}[\alpha\zeta_i] \end{pmatrix} \psi_i \right] \\ &+ \begin{pmatrix} 0 \\ \mathbb{E}[f] \end{pmatrix} \end{aligned} \tag{5}$$

$$\begin{aligned} \frac{\partial \zeta}{\partial t} &= -\langle \frac{\partial \overline{\Psi}}{\partial t}, \psi \rangle + \left\langle \begin{pmatrix} 0 & 1 \\ c^2(\nabla^2 - \nabla\phi^T\nabla) & -\alpha \end{pmatrix} \overline{\Psi}, \psi \right\rangle \\ &+ \sum_i \left[\zeta_i \left\langle \begin{pmatrix} 0 & 1 \\ c^2(\nabla^2 - \nabla\phi^T\nabla) & -\alpha \end{pmatrix} \psi_i, \psi \right\rangle \right] \\ &+ \left\langle \begin{pmatrix} 0 \\ f \end{pmatrix}, \psi \right\rangle \end{aligned} \tag{6}$$

$$\frac{\partial \psi}{\partial t} = \mathscr{P}_{\psi}^{\perp}[\mathcal{A}]\mathbf{C}_{\zeta\zeta^*}^{-1} \tag{7}$$

where we used the orthogonal projection operator $\mathscr{P}_{\psi}^{\perp}$, $\mathcal{A}$, and the covariance matrix $\mathbf{C}_{\zeta\zeta^*}$ defined below,

$$\mathscr{P}_{\psi}^{\perp}[\bullet] \equiv \bullet - \psi\langle\psi, \bullet\rangle \tag{8}$$

$$\begin{aligned} \mathcal{A} &\equiv \begin{pmatrix} 0 & 0 \\ \mathbb{E}[c^2\zeta^*] - \mathbb{E}[c^2\zeta\nabla\phi]\cdot & -\mathbb{E}[\alpha\zeta^*] \end{pmatrix} \overline{\Psi} \\ &+ \sum_i \left[\begin{pmatrix} 0 & \mathbb{E}[\zeta_i\zeta^*] \\ \mathbb{E}[c^2\zeta_i\zeta^*]\nabla^2 - \mathbb{E}[c^2\zeta_i\zeta^*\nabla\phi]\cdot\nabla & \mathbb{E}[\alpha\zeta_i\zeta^*] \end{pmatrix} \psi_i \right] \\ &+ \begin{pmatrix} 0 \\ \mathbb{E}[f\zeta^*] \end{pmatrix} \end{aligned} \tag{9}$$

$$\left(\mathbf{C}_{\zeta\zeta^*}\right)_{ij} \equiv \mathbb{E}[\zeta_i\zeta_j^*] \tag{10}$$

Note that ψ and ζ, when referenced without a subscript i, denote row vectors $(\psi_1, \psi_2, \ldots)$ and $(\zeta_1, \zeta_2, \ldots)$, respectively. A variable with * denotes the complex conjugate of the respective variable. The ijth element of the spatial inner product $\langle a, b\rangle$ between vector quantities a and b is defined $\langle a_i, b_j\rangle$, where a_i and b_j are scalar fields.

With these equations, one may spatially discretize and adopt a classic numerical time-integration scheme to numerically advance $\overline{\Psi}$, ψ, and ζ starting from initial conditions given by the singular value decomposition (see, e.g., [17], [18]). When doing so, one must be careful to rescale p and $\frac{\partial p}{\partial t}$ by the standard deviation or similar statistic of their respective distributions in the initial conditions; this non-dimensionalizes the system. Because p and $\frac{\partial p}{\partial t}$ share stochastic coefficients ζ, it is imperative to normalize by some statistic [36]–[38], otherwise a majority of the uncertainty may be falsely attributed to whichever variable is larger in magnitude.

Alternatively, the DO equations themselves may be discretized as in the dynamical low-rank approximation [29], and the discretized differential operator for the acoustic wave equation may be inserted to numerically solve the reduced-order model. For details of this methodology, see [15], [17], [31], [39]. Here, we will provide a brief overview. For a PDE of the form $\frac{\partial \Psi}{\partial t} = \mathscr{L}_c(\Psi, t; \eta)$, we seek a spatially discrete solution Ψ_d that can be represented in low-rank form: $\Psi_d(t) = U(t)Z(t)^T$. For a fixed time t, if $\Psi_d(t) \in \mathbb{R}^{m\times n}$, we insist that $U(t) \in \mathbb{R}^{m\times r}$ and $Z(t) \in \mathbb{R}^{n\times r}$ where $r \ll m, n$. This way, we save in storage due to the compressed form of Ψ_d and improve computational efficiency because of the reduced cost of matrix multiplications and inversions of smaller matrices in the time marching and computation of $\mathscr{L}_d$. The spatially discrete DO equations tell us how to instantaneously optimally evolve U and Z to follow the dynamics of $\mathscr{L}_d$ [15] and take the following form,

$$\begin{aligned} \dot{U} &= \mathscr{P}_U^{\perp}\mathscr{L}_d(UZ^T, t; \eta)Z(Z^TZ)^{-1} \\ \dot{Z} &= \mathscr{L}_d(UZ^T, t; \eta)^T U \end{aligned} \tag{11}$$

Here, $\mathscr{L}_d$ represents the spatially discretized version of the spatially continuous differential operator $\mathscr{L}_c$. $\mathscr{P}_U^{\perp} = I - UU^T$, and the columns of U, u_i, correspond to the modes ψ_i in (4). Similarly, the columns of Z, z_i, correspond to realizations of ζ_i. The discrete DO condition is now $\dot{U}^TU = 0$. Although the discrete DO equations do not explicitly extract the mean of Ψ_d, the mean may be included by adding a column in U and a column of ones in Z. An important difference between the spatially and discrete DO equations is that the spatially

continuous version is intrusive, requiring a new derivation for each PDE, whereas the spatially discrete version is non-intrusive. This is evident in the simplicity of equations (11).

For our problem of interest, we would simply discretize (12) using a finite difference/volume/element scheme to find $\mathscr{L}_d$ and insert it into (11) to find our coupled system of ODEs. Integrating these ODEs in time is no trivial task; this is a coupled set of nonlinear equations that can become unstable if treated improperly: the system may become ill-conditioned, U must be re-orthonormlized [40], and retraction error could cause overshoot [39], among other technicalities. We refer the reader to [31], [39], [41] for examples on how to integrate these equations in a stable and high-order manner.

III. Reduced-order stochastic acoustic wave equation

Using the discrete DO equations, we implement a test case meant to simulate 2D acoustic propagation in an uncertain ocean with a bumpy bathymetry as shown in figures 1-6. For better stability properties, we discretize the density-reduced acoustic wave equation below, where we solve for the variable $\tilde{\Psi} = \Psi/\rho$, and then multiply by $\sqrt{\rho}$ at the end to get back to the original variables.

$$\frac{\partial \tilde{\Psi}}{\partial t} = \begin{pmatrix} 0 & 1 \\ c^2\left[\nabla^2 + \frac{\nabla^2\rho}{2\rho} - \frac{3(\nabla\rho)\cdot(\nabla\rho)}{4\rho^2}\right] & -\alpha \end{pmatrix} \tilde{\Psi} + \begin{pmatrix} 0 \\ \frac{f}{\sqrt{\rho}} \end{pmatrix} \quad (12)$$

We use a 75 Hz point source at a range and depth of 50m with Gaussian time-window, shown in Figure 1. The density of the water (above the white border in figures 3-6) is 1000 kg/m^3, and the density of the ocean floor (below the white border) is 1500 kg/m^3. The ocean sound speed is given by the Mackenzie profile [42] at 15°C and 30 ppt salinity augmented with stochastic constant, linear, and quadratic (in depth) terms weighted by normal random variables. The ocean bottom has a sound speed of 1700 m/s. The decay term α is set to zero in the computational domain of interest for this example. The sharp discontinuity in density and sound speed at the ocean bottom creates an impedance boundary where some of the energy is reflected back to the surface, where we use a pressure-release (Dirichlet-zero) boundary. All other boundaries are open and implemented with an absorbing boundary layer (not shown). We use a rank-5 simulation, i.e. five DO modes, to represent the solution with 1000 stochastic realizations on a 201×201 grid (excluding the absorbing boundary layers). To advance $\mathscr{L}_d$ in time, we use a classic leapfrog scheme, and we couple this with the projector-splitting integrator used as a retraction from [41]. For the spatial derivatives, we use second-order central differences.

Figure 2 shows the received signal at a range of 100m and a depth of 10m for each of the 1000 realizations. We see that the signal is appropriately delayed with some change in shape from the original pulse due to the reflection off of the surface. The next pulse is the reflection off of the ocean bottom; most of the energy is transmitted through the ground and geometrically dispersed, so the reflected pulse is much weaker. However, there is increased stochastic variability because the pulses have traveled a longer distance through the stochastic medium.

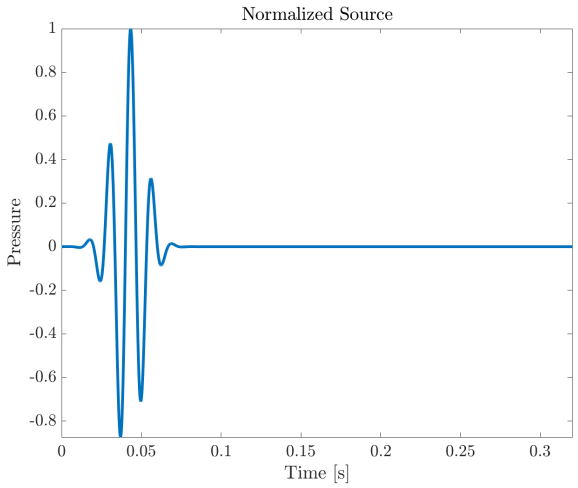

Fig. 1. Normalized source signal

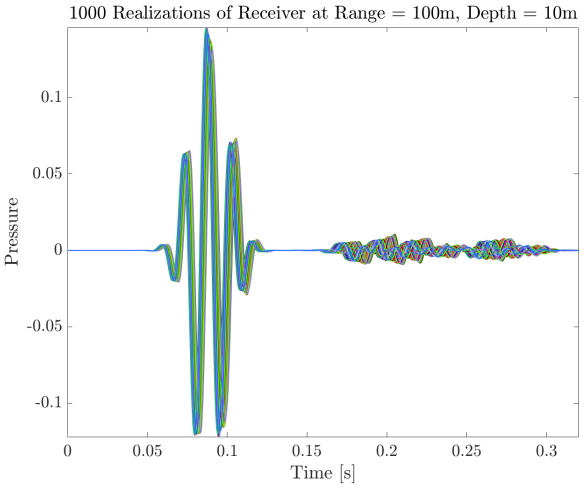

Fig. 2. Received signal with stochastic variation

Figures 3-6 show the mean of the DO solution at various points in time. First we see the pulse propagate outwards. Then, it bounces off of the air-water interface later makes contact with the ocean bottom. Some of the energy at the bottom is reflected back to the surface, where it is reflected back, creating an interference pattern. Although we only display the mean of the solution, we note that any of the 1000 realizations may be easily reconstructed and visualized. Similarly, varied statistics of the stochastic acoustic wave can be easily evaluated. This includes fields of standard deviation, kurtosis, and other moments, as well as mutual information fields and other probabilistic forecasts [6], [23], [43].

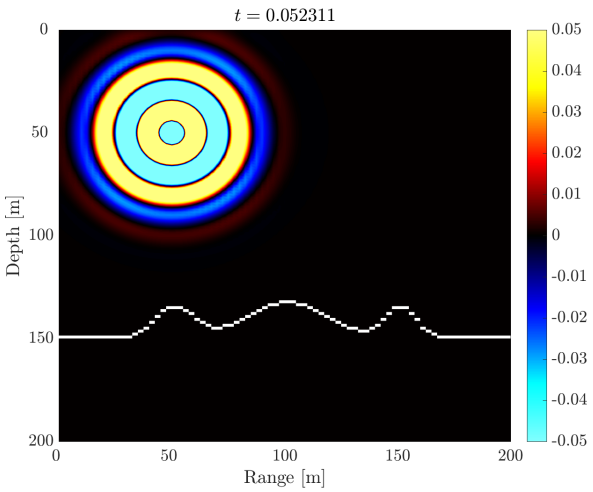

Fig. 3. Mean of DO solution at time t_1

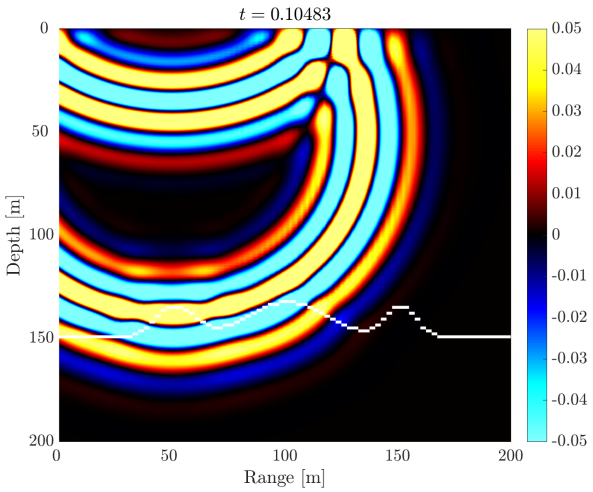

Fig. 4. Mean of DO solution at time t_2

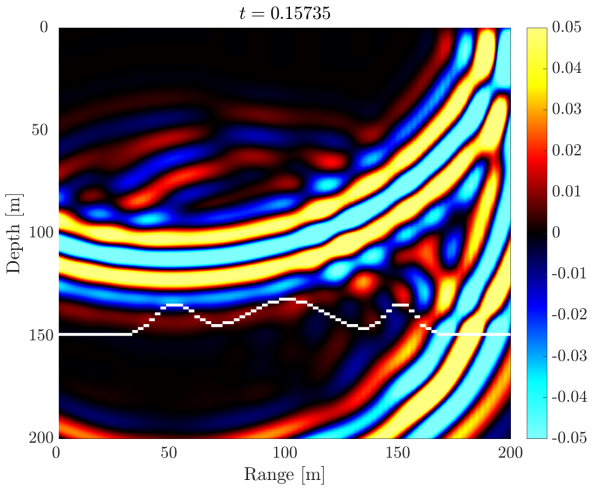

Fig. 5. Mean of DO solution at time t_3

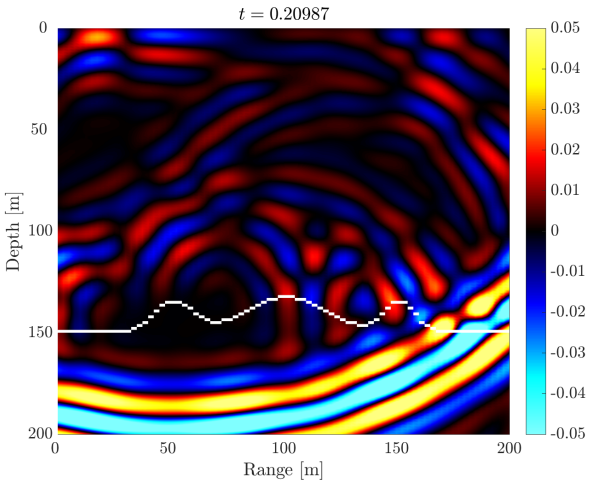

Fig. 6. Mean of DO solution at time t_4

IV. Reduced-order Deterministic 3D parabolic wave equation

In this section we apply the dynamical low-rank approximation to the three-dimensional deterministic parabolic wave equation. In previous work, the DO equations have been applied to reduce the *stochastic* dimensionality of the system. Here, we reduce the *deterministic* dimensionality with the same DO methodology but with a slightly different viewpoint. This saves computational time and storage when solving 3D acoustic forward models.

We start with the density-reduced 3D parabolic/paraxial acoustic wave equation in Cartesian coordinates.

$$\frac{\partial \phi}{\partial x} = \left[\frac{ik_0}{2}(\tilde{n}^2 - 1) + \frac{i}{2k_0}\left(\frac{\partial^2}{\partial y^2} + \frac{\partial^2}{\partial z^2} \right) \right] \phi \tag{13}$$

The effective index of refraction $\tilde{n}$ is given by the index of refraction n and the density ρ as follows.

$$\tilde{n}^2 = n^2 + \frac{1}{2k_0^2}\left[\frac{\nabla^2 \rho}{\rho} - \frac{3(\nabla \rho) \cdot (\nabla \rho)}{2\rho^2} \right] \tag{14}$$

Recall that to recover the pressure from the density-reduced parabolic equation, we use the relation $p(x, y, z) = \phi(x, y, z) e^{ik_0 x} \sqrt{\rho}$ where k_0 is a reference wavenumber for the media. In a similar fashion to normal-mode methods [12], we assume that the solution ϕ can be decomposed as follows,

$$\phi(x, y, z) = \sum_i \mathcal{Y}_i(x, y) \mathcal{Z}_i(x, z) \tag{15}$$

This decomposition is valid assuming ϕ is square-integrable [44], which is essentially always the case for physical problems. In contrast to normal-mode methods, we allow $\mathcal{Y}$ and $\mathcal{Z}$ to evolve in range, x. And to evolve $\mathcal{Y}$ and $\mathcal{Z}$, we employ the dynamical low-rank approximation (or the spatially discrete DO equations) which gives us instantaneously optimal differential equations. The only difference from the results of the prior Sections II-III is that instead of having deterministic modes and stochastic coefficients that evolve in time, we have

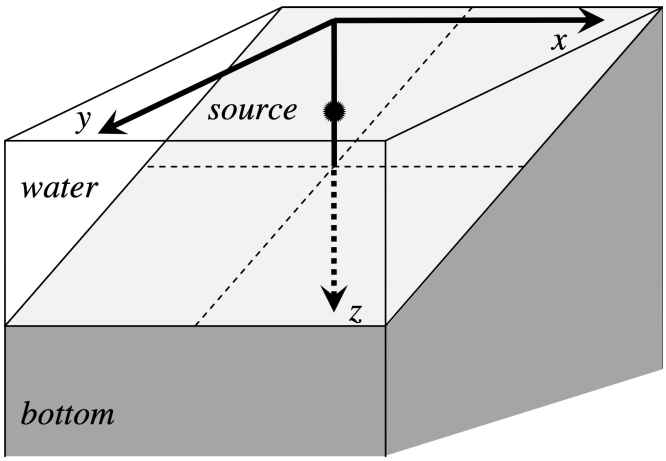

Fig. 7. Wedge test case geometry from [45] with a 5° slope

two sets of deterministic modes that evolve in range. One way to reason through the difference between (4) and (15) is to replace $\zeta \in \Omega$, a simple event in the stochastic event space, with $z \in \mathbb{R}$. Then, in the discrete formulation, the $\mathcal{Y}$ modes are mapped to the matrix U, and the $\mathcal{Z}$ modes are mapped to the matrix Z in (11).

We illustrate this new adaptive reduced-order deterministic methodology through example of a 3D wedge test case from [45]. The problem geometry is depicted in Figure 7 with an artificial absorption layer (not shown). The water sound speed is set to 1475 m/s whereas the bottom sound speed is set to 1700 m/s. Additionally, the water has density $1{,}000$ kg/m^3 and the ocean bottom has density $1{,}500$ kg/m^3. The water has no absorption, but the ocean bottom has an absorption of 0.5 dB per wavelength. To implement the absorption, we utilize a complex index of refraction. We solve over a 25 km $\times$ 4 km $\times$ 0.5 km domain with $166,667$ points in x, 2,867 points in y, and 650 points in z, for a total of about 3.1059×10^{11} grid points. We discretize x finely to ensure the scheme remains stable. For simplicity, we use a modified Greene's source [46] at 75 Hz as our starter, though a more realistic 3D starter may be used in the future rather than this 3D adaptation of a 2D starter,

$$\phi(0,y,z) = \sqrt{k_0}\left(1.4467 - 0.4201k_0^2(z-100)^2y^2\right) \cdot e^{-k_0^2\frac{(z-100)^2}{3.0512}} e^{-k_0^2\frac{y^2}{3.0512}} \quad (16)$$

We solve this equation with a central differences in space and a Dufort-Frankel scheme [47] in time at ranks 5 and 20 using our reduced-order scheme with the projector-splitting retraction [41], and at full-rank, 650, using the traditional discretized integration scheme.

In Figure 8, we show slices of the 3D solution with the dynamical low-rank reduced-order deterministic DO methodology at ranks 5 and 20 as well as the full-rank solution. We find that at rank-5, the solution is significantly different from the full-rank solution, though it still looks physical, which is an advantage of this reduced-order method. At rank-20, the

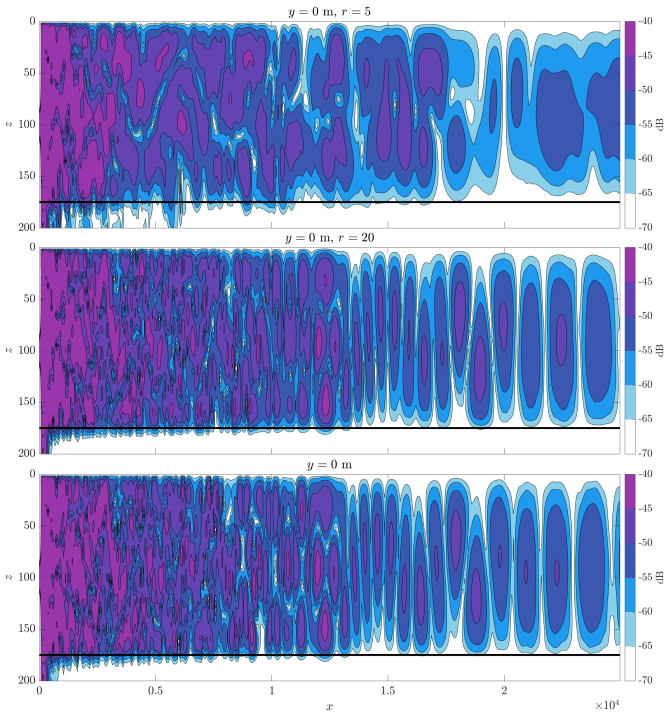

Fig. 8. Solution slices of the density-reduced pressure ϕ at $y = 0$ of wedge test case, using the adaptive reduced-order deterministic DO equations at rank $r = 5$ and $r = 20$ compared with the full-rank, $r = 650$, solution.

solution looks very close to the full-rank solution; this implies that a low-rank adaptive deterministic DO approximation of the solution converges quickly to the full-rank solution.

This approach may be useful when the three-dimensional computational mesh is particularly large and, without compression from the dynamical low-rank approximation, storage in memory or even a hard drive is infeasible. As a result, the DO deterministic approach is also particularly useful for acoustic computation both for and onboard autonomous underwater vehicles (AUVs) in real-time operations [48]–[51] as well as for several new ocean acoustics applications [52]–[54].

V. Conclusion and Future Work

We have developed two new frameworks for forward modeling in ocean acoustics. The first is to model the stochastic wave equation with the newly derived DO differential equations (5-7). This serves as an efficient alternative to stochastic wave Monte Carlo simulations and may be used for non-Gaussian uncertainty quantification and predicting complex scattering phenomena. We demonstrate its efficacy on a 2D test case of an acoustic pulse propagating through uncertain media, reflecting off of the air-ocean interface and bumpy bathymetry. By reconstructing realizations, we are able to evaluate any statistics desired from the solution distribution. The second framework is to use the DO equations on the deterministic parabolic wave equation. This approach is similar in spirit to the normal modes approach [12], but here the modes optimally evolve in range according to the dynamics of the PDE to give the best low-rank approximation rather than remain fixed

a priori. This gives an accurate and efficient method for solving deterministic 3D ocean acoustic problems with weak scattering. For this case, we solve a 3D wedge test case and show that low-rank solutions converge quickly to the full-rank solution.

Future work include exploring additional acoustic approximations, e.g. low-rank ray and Eikonal methods. One may also couple models, e.g. the full wave equation and the parabolic wave equation, using the full wave equation near areas with discontinuities in sound speed, density, or absorption, and using the parabolic wave equation in regions with smooth parameters (i.e. when scattering is weak). Finally, one can apply these forward models as very efficient approximations to the steepest descent direction in the adjoint-state method to form an image.

ACKNOWLEDGMENT

The authors would like to thank the MSEAS group members for their contributions, especially Mr. Wael Hajj Ali and Mr. Manmeet Singh Bhabra. We also thank the Office of Naval Research for partial support under grants N00014-19-1-2693 (IN-BDA) and N00014-19-1-2664 (Task Force Ocean, DEEP-AI).

REFERENCES

[1] L. Mayer, M. Jakobsson, G. Allen, B. Dorschel, R. Falconer, V. Ferrini, G. Lamarche, H. Snaith, and P. Weatherall, "The nippon foundation—gebco seabed 2030 project: The quest to see the world's oceans completely mapped by 2030," *Geosciences*, vol. 8, no. 2, 2018. [Online]. Available: https://www.mdpi.com/2076-3263/8/2/63

[2] C.-F. Huang, P. Gerstoft, and W. S. Hodgkiss, "Effect of ocean sound speed uncertainty on matched-field geoacoustic inversion," *The Journal of the Acoustical Society of America*, vol. 123, no. 6, pp. EL162–EL168, 2008. [Online]. Available: https://doi.org/10.1121/1.2908406

[3] Y.-M. Jiang and N. R. Chapman, "The impact of ocean sound speed variability on the uncertainty of geoacoustic parameter estimates," *The Journal of the Acoustical Society of America*, vol. 125, no. 5, pp. 2881–2895, 2009. [Online]. Available: https://asa.scitation.org/doi/abs/10.1121/1.3097770

[4] M. Siderius, P. L. Nielsen, J. Sellschopp, M. Snellen, and D. Simons, "Experimental study of geo-acoustic inversion uncertainty due to ocean sound-speed fluctuations," *The Journal of the Acoustical Society of America*, vol. 110, no. 2, pp. 769–781, 2001. [Online]. Available: https://doi.org/10.1121/1.1385898

[5] A. B. Baggeroer, W. A. Kuperman, and P. N. Mikhalevsky, "An overview of matched field methods in ocean acoustics," *IEEE Journal of Oceanic Engineering*, vol. 18, no. 4, pp. 401–424, 1993.

[6] P. F. J. Lermusiaux and C.-S. Chiu, "Four-dimensional data assimilation for coupled physical-acoustical fields," in *Acoustic Variability, 2002*, N. G. Pace and F. B. Jensen, Eds. Saclantcen: Kluwer Academic Press, 2002, pp. 417–424.

[7] A. R. Robinson and P. F. J. Lermusiaux, "Prediction systems with data assimilation for coupled ocean science and ocean acoustics," in *Proceedings of the Sixth International Conference on Theoretical and Computational Acoustics*, A. Tolstoy et al, Ed. World Scientific Publishing, 2004, pp. 325–342, refereed invited Keynote Manuscript.

[8] P. F. J. Lermusiaux, J. Xu, C.-F. Chen, S. Jan, L. Chiu, and Y.-J. Yang, "Coupled ocean–acoustic prediction of transmission loss in a continental shelfbreak region: Predictive skill, uncertainty quantification, and dynamical sensitivities," *IEEE Journal of Oceanic Engineering*, vol. 35, no. 4, pp. 895–916, Oct. 2010.

[9] C. Evangelinos, P. F. J. Lermusiaux, J. Xu, P. J. Haley, and C. N. Hill, "Many task computing for real-time uncertainty prediction and data assimilation in the ocean," *IEEE Transactions on Parallel and Distributed Systems*, vol. 22, no. 6, pp. 1012–1024, Jun. 2011, Special Section on Many-Task Computing.

[10] T. F. Duda, Y.-T. Lin, A. E. Newhall, K. R. Helfrich, W. G. Zhang, M. Badiey, P. F. J. Lermusiaux, J. A. Colosi, and J. F. Lynch, "The "Integrated Ocean Dynamics and Acoustics" (IODA) hybrid modeling effort," in *Proceedings of the international conference on Underwater Acoustics - 2014 (UA2014)*, 2014, pp. 621–628.

[11] T. F. Duda, Y.-T. Lin, A. E. Newhall, K. R. Helfrich, J. F. Lynch, W. G. Zhang, P. F. J. Lermusiaux, and J. Wilkin, "Multiscale multiphysics data-informed modeling for three-dimensional ocean acoustic simulation and prediction," *Journal of the Acoustical Society of America*, vol. 146, no. 3, pp. 1996–2015, Sep. 2019.

[12] F. B. Jensen, W. A. Kuperman, M. B. Porter, and H. Schmidt, *Computational ocean acoustics*. Springer Science & Business Media, 2011.

[13] R.-E. Plessix, "A review of the adjoint-state method for computing the gradient of a functional with geophysical applications," *Geophysical Journal International*, vol. 167, no. 2, pp. 495–503, 2006.

[14] J. Virieux and S. Operto, "An overview of full-waveform inversion in exploration geophysics," *Geophysics*, vol. 74, no. 6, pp. WCC1–WCC26, 2009.

[15] F. Feppon and P. F. J. Lermusiaux, "A geometric approach to dynamical model-order reduction," *SIAM Journal on Matrix Analysis and Applications*, vol. 39, no. 1, pp. 510–538, 2018.

[16] T. P. Sapsis and P. F. J. Lermusiaux, "Dynamically orthogonal field equations for continuous stochastic dynamical systems," *Physica D: Nonlinear Phenomena*, vol. 238, no. 23–24, pp. 2347–2360, Dec. 2009.

[17] F. Feppon and P. F. J. Lermusiaux, "Dynamically orthogonal numerical schemes for efficient stochastic advection and Lagrangian transport," *SIAM Review*, vol. 60, no. 3, pp. 595–625, 2018.

[18] M. P. Ueckermann, P. F. J. Lermusiaux, and T. P. Sapsis, "Numerical schemes for dynamically orthogonal equations of stochastic fluid and ocean flows," *Journal of Computational Physics*, vol. 233, pp. 272–294, Jan. 2013.

[19] D. N. Subramani, "Probabilistic regional ocean predictions: Stochastic fields and optimal planning," Ph.D. dissertation, Massachusetts Institute of Technology, Department of Mechanical Engineering, Cambridge, Massachusetts, Feb. 2018.

[20] D. Subramani and P. F. J. Lermusiaux, "Probabilistic ocean predictions with dynamically-orthogonal primitive equations," 2020, in preparation.

[21] K. A. Gkirgkis, "Stochastic ocean forecasting with the dynamically orthogonal primitive equations," Master's thesis, Massachusetts Institute of Technology, Department of Mechanical Engineering, Cambridge, Massachusetts, Jun. 2021.

[22] D. N. Subramani and P. F. J. Lermusiaux, "Energy-optimal path planning by stochastic dynamically orthogonal level-set optimization," *Ocean Modeling*, vol. 100, pp. 57–77, 2016.

[23] P. F. J. Lermusiaux, D. N. Subramani, J. Lin, C. S. Kulkarni, A. Gupta, A. Dutt, T. Lolla, P. J. Haley, Jr., W. H. Ali, C. Mirabito, and S. Jana, "A future for intelligent autonomous ocean observing systems," *Journal of Marine Research*, vol. 75, no. 6, pp. 765–813, Nov. 2017, the Sea. Volume 17, The Science of Ocean Prediction, Part 2.

[24] D. N. Subramani, P. J. Haley, Jr., and P. F. J. Lermusiaux, "Energy-optimal path planning in the coastal ocean," *Journal of Geophysical Research: Oceans*, vol. 122, pp. 3981–4003, 2017.

[25] D. N. Subramani and P. F. J. Lermusiaux, "Risk-optimal path planning in stochastic dynamic environments," *Computer Methods in Applied Mechanics and Engineering*, vol. 353, pp. 391–415, Aug. 2019.

[26] W. H. Ali, M. S. Bhabra, P. F. J. Lermusiaux, A. March, J. R. Edwards, K. Rimpau, and P. Ryu, "Stochastic oceanographic-acoustic prediction and Bayesian inversion for wide area ocean floor mapping," in *OCEANS 2019 MTS/IEEE SEATTLE*. Seattle: IEEE, Oct. 2019, pp. 1–10.

[27] W. H. Ali and P. F. J. Lermusiaux, "Dynamically orthogonal equations for stochastic underwater sound propagation: Theory, schemes and applications," 2021, in preparation.

[28] ——, "Acoustics Bayesian inversion with Gaussian mixture models using the dynamically orthogonal field equations," 2021, in preparation.

[29] O. Koch and C. Lubich, "Dynamical low-rank approximation," *SIAM Journal on Matrix Analysis and Applications*, vol. 29, no. 2, pp. 434–454, 2007. [Online]. Available: https://doi.org/10.1137/050639703

[30] F. Feppon and P. F. J. Lermusiaux, "The extrinsic geometry of dynamical systems tracking nonlinear matrix projections," *SIAM Journal on Matrix Analysis and Applications*, vol. 40, no. 2, pp. 814–844, 2019.

[31] A. Charous, "High-order retractions for reduced-order modeling and uncertainty quantification," Master's thesis, Massachusetts Institute of Technology, Center for Computational Science and Engineering, Cambridge, Massachusetts, Feb. 2021.

[32] E. Musharbash, "Dynamical low rank approximation of pdes with random parameters," EPFL, Tech. Rep., 2017.
[33] E. Musharbash, F. Nobile, and E. Vidličková, "Symplectic dynamical low rank approximation of wave equations with random parameters," *BIT Numerical Mathematics*, pp. 1–49, 2017.
[34] K. Karhunen, *Über lineare Methoden in der Wahrscheinlichkeitsrechnung*. Sana, 1947, vol. 37.
[35] M. Loéve, *Probability Theory II*, 4th ed., ser. Graduate Texts in Mathematics. Springer-Verlag New York, 1978, vol. 2.
[36] P. F. J. Lermusiaux and A. R. Robinson, "Data assimilation via Error Subspace Statistical Estimation, part I: Theory and schemes," *Monthly Weather Review*, vol. 127, no. 7, pp. 1385–1407, 1999.
[37] P. F. J. Lermusiaux, "Data assimilation via Error Subspace Statistical Estimation, part II: Mid-Atlantic Bight shelfbreak front simulations, and ESSE validation," *Monthly Weather Review*, vol. 127, no. 7, pp. 1408–1432, Jul. 1999.
[38] ——, "Estimation and study of mesoscale variability in the Strait of Sicily," *Dynamics of Atmospheres and Oceans*, vol. 29, no. 2, pp. 255–303, 1999.
[39] A. Charous and P. F. J. Lermusiaux, "Perturbative retractions with high-order convergence to the best low-rank approximation," *SIAM Journal on Scientific Computing*, 2021, sub-judice.
[40] J. Lin and P. F. J. Lermusiaux, "Minimum-correction second-moment matching: Theory, algorithms and applications," *Numerische Mathematik*, vol. 147, no. 3, pp. 611–650, Mar. 2021.
[41] C. Lubich and I. V. Oseledets, "A projector-splitting integrator for dynamical low-rank approximation," *BIT Numerical Mathematics*, vol. 54, no. 1, pp. 171–188, 2014.
[42] K. V. Mackenzie, "Nine-term equation for sound speed in the oceans," *The Journal of the Acoustical Society of America*, vol. 70, no. 3, pp. 807–812, 1981. [Online]. Available: https://doi.org/10.1121/1.386920
[43] P. F. J. Lermusiaux, P. J. Haley, Jr., S. Jana, A. Gupta, C. S. Kulkarni, C. Mirabito, W. H. Ali, D. N. Subramani, A. Dutt, J. Lin, A. Shcherbina, C. Lee, and A. Gangopadhyay, "Optimal planning and sampling predictions for autonomous and Lagrangian platforms and sensors in the northern Arabian Sea," *Oceanography*, vol. 30, no. 2, pp. 172–185, Jun. 2017, special issue on Autonomous and Lagrangian Platforms and Sensors (ALPS).
[44] J. Šimša, "The best l2-approximation by finite sums of functions with separable variables," *Aequationes mathematicae*, vol. 43, no. 2-3, pp. 248–263, 1992.
[45] Y.-T. Lin, T. F. Duda, and A. E. Newhall, "Three-dimensional sound propagation models using the parabolic-equation approximation and the split-step fourier method," *Journal of Computational Acoustics*, vol. 21, no. 01, p. 1250018, 2013.
[46] R. R. Greene, "The rational approximation to the acoustic wave equation with bottom interaction," *The Journal of the Acoustical Society of America*, vol. 76, no. 6, pp. 1764–1773, 1984. [Online]. Available: https://doi.org/10.1121/1.391561
[47] B. Gustafsson, H. Kreiss, and J. Oliger, *Time Dependent Problems and Difference Methods*, ser. A Wiley-Interscience Publication. Wiley, 1995. [Online]. Available: https://books.google.com/books?id=1JZ2mSQ-O6MC
[48] J. Xu, P. F. J. Lermusiaux, P. J. Haley Jr., W. G. Leslie, and O. G. Logutov, "Spatial and Temporal Variations in Acoustic propagation during the PLUSNet-07 Exercise in Dabob Bay," in *Proceedings of Meetings on Acoustics (POMA)*, vol. 4. Acoustical Society of America 155th Meeting, 2008, p. 11.
[49] D. Wang, P. F. J. Lermusiaux, P. J. Haley, Jr., D. Eickstedt, W. G. Leslie, and H. Schmidt, "Acoustically focused adaptive sampling and on-board routing for marine rapid environmental assessment," *Journal of Marine Systems*, vol. 78, no. Supplement, pp. S393–S407, Nov. 2009.
[50] M. E. G. D. Colin, T. F. Duda, L. A. te Raa, T. van Zon, P. J. Haley, Jr., P. F. J. Lermusiaux, W. G. Leslie, C. Mirabito, F. P. A. Lam, A. E. Newhall, Y.-T. Lin, and J. F. Lynch, "Time-evolving acoustic propagation modeling in a complex ocean environment," in *OCEANS - Bergen, 2013 MTS/IEEE*, 2013, pp. 1–9.
[51] J. P. Heuss, P. J. Haley, Jr., C. Mirabito, E. Coelho, M. C. Schönau, K. Heaney, and P. F. J. Lermusiaux, "Reduced order modeling for stochastic prediction onboard autonomous platforms at sea," in *OCEANS 2020 IEEE/MTS*. IEEE, Oct. 2020, pp. 1–10.
[52] F.-P. A. Lam, P. J. Haley, Jr., J. Janmaat, P. F. J. Lermusiaux, W. G. Leslie, M. W. Schouten, L. A. te Raa, and M. Rixen, "At-sea real-time coupled four-dimensional oceanographic and acoustic forecasts during Battlespace Preparation 2007," *Journal of Marine Systems*, vol. 78, no. Supplement, pp. S306–S320, Nov. 2009.
[53] P. F. J. Lermusiaux, C. Mirabito, P. J. Haley, Jr., W. H. Ali, A. Gupta, S. Jana, E. Dorfman, A. Laferriere, A. Kofford, G. Shepard, M. Goldsmith, K. Heaney, E. Coelho, J. Boyle, J. Murray, L. Freitag, and A. Morozov, "Real-time probabilistic coupled ocean physics-acoustics forecasting and data assimilation for underwater GPS," in *OCEANS 2020 IEEE/MTS*. IEEE, Oct. 2020, pp. 1–9.
[54] P. F. J. Lermusiaux, P. J. Haley, Jr., C. Mirabito, W. H. Ali, M. Bhabra, P. Abbot, C.-S. Chiu, and C. Emerson, "Multi-resolution probabilistic ocean physics-acoustic modeling: Validation in the New Jersey continental shelf," in *OCEANS 2020 IEEE/MTS*. IEEE, Oct. 2020, pp. 1–9.